Interfacial Reaction of Pb-Sn Solder and Sn-Ag Solder with Electroless Ni Deposit during Reflow

M.O. ALAM,[1] Y.C. CHAN,[1,2] and K.C. HUNG[1]

1.—Department of Electronic Engineering, City University of Hong Kong, Hong Kong. 2.—E-mail: EEYCCHAN@cityu.edu.hk

The interfaces between electroless Ni-P deposit and Pb-Sn solder and Sn-Ag solder were formed by reflowing for different time periods to examine their microstructures and microchemistry. It was found that the Pb-Sn solder interface is more stable than the Sn-Ag solder interface. Sn-Ag solder reacts quickly with the electroless Ni-P deposit and forms nonadherent Ni-Sn intermetallic compounds (IMCs). Pb-Sn solder reacts slowly and forms adherent Ni-Sn IMC. A P-rich Ni layer, revealed as a dark layer under scanning electron microscopy (SEM), is formed on the electroless Ni-P deposit due to the solder reaction. For short reflow times, this P-rich Ni layer consists of only Ni_3P compound, but during prolonged reflow, new crystals of Ni_2P, Ni_5P_4, and NiP_2 are also found to be formed from the amorphous electroless Ni-P layer.

Key words: Reflow, electroless Ni-P, intermetallic compound, amorphous, crystallization

INTRODUCTION

Soldering technology using Pb-Sn solders still plays an important role in electronic packaging, such as flip-chip, solder-ball connections in ball grid array (BGA), and integrated circuit assembly to a printed circuit board (PCB).[1,2] However, from the environmental point of view, Pb-containing solders are harmful to the environment and human beings. The investigation of Pb-free solder has been intensified recently due to the anticipated legislation to ban the use of Pb in electrical and electronic products.[3–6] Of all the Pb-free solders, Sn-based solders are the most attractive materials for the replacement of Pb-Sn solder. Tin fulfils the metallurgical, environmental, economic, and supply criteria, and therefore most of the effort has been directed toward Sn-containing binary or ternary alloys.[7,8]

Copper is widely used in the under bump metallurgy and substrate metallization for flip-chip and BGA applications. The interaction and interdiffusion behaviors between solder and Cu-base metal have been intensively studied. It is now known that at the Cu/solder interface, Sn reacts rapidly with Cu to form Cu-Sn intermetallic compound (IMC), which weakens the solder joints due to the brittle nature of the IMC. The strength of the solder joint decreases with increasing thickness of IMC formed at the interface and the IMC acts as an initiation site for microcracks.[9–11] It is found that the growth rate of IMCs is greater in the Cu/solder system than in the Ni/solder. Nickel is thus recognized to act as a diffusion barrier between Cu and solder in order to sustain a long period of service.[11] Characteristics of the electroless Ni deposit such as excellent solderability, corrosion resistance, uniform thickness, and selective deposition make the electroless Ni plating more suitable as a material for a diffusion barrier than pure electrodeposited Ni.[12–14] However, very little work has been performed on the interaction and interdiffusion behavior of electronic solder alloys and electroless Ni-P.

Recently, Jang et al.[12] and Hung et al.[13] reported solder reaction-assisted crystallization of electroless Ni-P to form Ni_3Sn_4 and Ni_3P compound at the interface when electroless Ni-P reacts with solder. Inaba et al.[15] found different Ni-Sn IMCs, Ni_2P, and NiP_2 at the solder/electroless Ni-P layer. In this work, we have studied the solder reaction in electroless Ni-P metallization during reflow soldering for both Pb-Sn solder and Pb-free solder. We have also investigated the growth of Ni-Sn intermetallics and subsequent changes in the Ni-P layers. The differences of the growth mechanisms have been

(Received March 25, 2002; accepted July 15, 2002)

explained for Pb-free solder with respect to Pb-Sn solder.

EXPERIMENTAL PROCEDURES

The test substrate was a custom-made FR4 PCB in which electroless Ni-P was deposited on a Cu pad. Immersion Au was immediately plated on top of the electroless Ni-P to avoid oxidation of the Ni surface. In order to maintain close to the optimum concentration of the plating solution and to ensure the optimum deposit quality, a complete automatic titration setup was used to monitor the content, the pH value, and the plating temperature, in the plating tanks. The P content in the electroless Ni substrate was controlled by the pH value of the plating solution. The thickness of the deposit layers was measured by using x-ray fluorescence (XRF) equipment or a Rutherford backscattering spectrometer (RBS), and the surface oxide or interface oxide in the substrates was detected by using oxygen resonance with a 3.04 MeV He^{++} ion beam. Eutectic 63Pb-37Sn solder balls and eutectic 96.5Sn-3.5Ag solder balls with a diameter of 0.75 mm were placed on the prefluxed Au/Ni-P/Cu pad substrates and reflowed at a temperature of 240°C for different reflow times from 0.5 min to 180 min. The flux was a no-clean flux.

For interfacial microstructure examination, the samples were mounted in epoxy and then sectioned using a slow speed diamond saw. The cross-sectioned samples were ground and polished carefully for scanning electron microscopy (SEM) study. The chemical and microstructural analyses of the cross-sectioned samples were obtained by using a scanning electron microscope with energy-dispersive x-ray analysis (EDX). The IMCs were identified by x-ray diffraction (XRD). The XRD analysis was conducted with a Cu target and a Ni filter at a scanning speed of 2°/min.

RESULTS

The cross section of Au/electroless Ni-P/Cu before reflow is shown in Fig. 1. The surface and interfaces of Au and electroless Ni-P are more or less smooth. Gold thickness of the Au/Ni-P/Cu pad is found to be around as 0.5 μm. The RBS result shows that there is no surface oxide and interface oxide in this raw Au/Ni-P/Cu substrate. The thickness of the Ni-P layer is around 3 μm, and the chemical composition of this layer, studied by EDX analysis, is found to be 80at.%Ni and 20at.%P. The thickness of the Cu layer is 15 μm. The XRD diffraction spectrum on the Au/electroless Ni-P/Cu before reflow shows only Cu and Au peaks—neither a peak of Ni nor Ni compound has been found. This finding proves that the electroless Ni-P was amorphous before reflow.

The reflow time in industrial applications rarely goes longer than 5 min. However, in this study, we used reflow time as long as 180 min. The sole purpose of using this prolong reflow time is to establish a kinetic database for Pb-free soldering on the electroless Ni-P deposit and to compare that with the

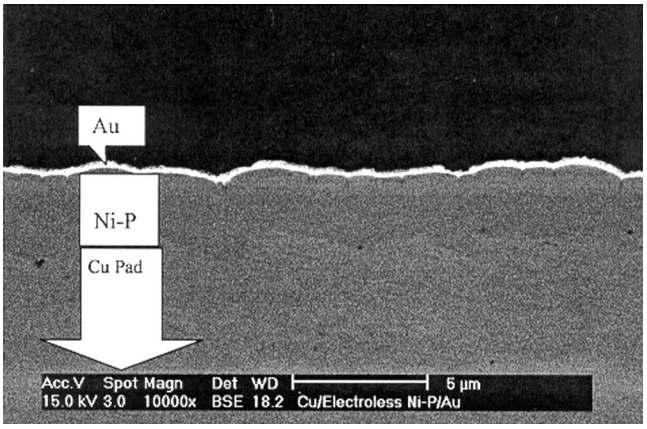

Fig. 1. Backscattered electron micrograph showing the cross section of a Au/electroless Ni-P/Cu pad before reflow.

conventional Pb-Sn solder. Figure 2 represents backscattered electron micrographs for the interfaces of Pb-Sn and Sn-Ag solder ball on electroless Ni-P after reflow at 240°C with different reflow times. These are cross-sectional micrographs with the section plane perpendicular to the faces of the substrates. From the micrographs of short reflow time, there are four layers from top to bottom—the solidified solder, reaction zone, Ni-P original layer, and Cu pad. The Au layer disappeared quickly; it dissolved in the molten solder within 30 sec. The EDX results at the interface confirmed that neither Au nor Au-Sn IMC layers were found at the interface. For 0.5 min reflow time, EDX analysis of the reaction zone revealed that the IMC is Ni_3Sn_4, which is also confirmed by other investigators.[12–18] A dark layer was observed between the Ni_3Sn_4 IMC and Ni-P layer from all SEM images. The EDX analysis showed that the P percentage of this dark layer at 0.5 min reflow is about 25 at.%. This finding implies that this dark layer at 0.5 min reflow time is composed of Ni_3P compound. The thicknesses of the Ni-Sn IMC layer and the P-enriched dark Ni-P layer increase with reflow time, whereas the thickness of the original Ni-P layer decreases. For Sn-Ag solder, the growth rates of Ni-Sn IMC and dark Ni-P layer are much faster.

From Fig. 2ia, the Pb-Sn solder interface contains needle and fine chunky Ni_3Sn_4 IMC at 0.5 min reflow. A very thin P-rich dark Ni-P layer (0.34 μm) formed adjacent to this Ni_3Sn_4 IMC. For the Sn-Ag solder interface at 0.5 min reflow (Fig. 2ib), the extent of Ni_3Sn_4 IMC formation is greater and hence the P-rich dark Ni-P layer is also thicker (0.93 μm). The thick Ni-Sn IMC layer is clear in Pb-Sn solder reflowed at 30 min (Fig 2iia). However, for the Sn-Ag solder interface (Fig. 2iib), some IMC grains detached from the interface after 30 min reflow. A thin continuous Ni-Sn IMC layer still adheres to the P-rich dark Ni-P layer. The P-rich dark layer is fractured and the original Ni-P layer is not visible (i.e., more Ni is consumed to form Ni-Sn IMC and the P is concentrated in the dark Ni-P layer). The EDX

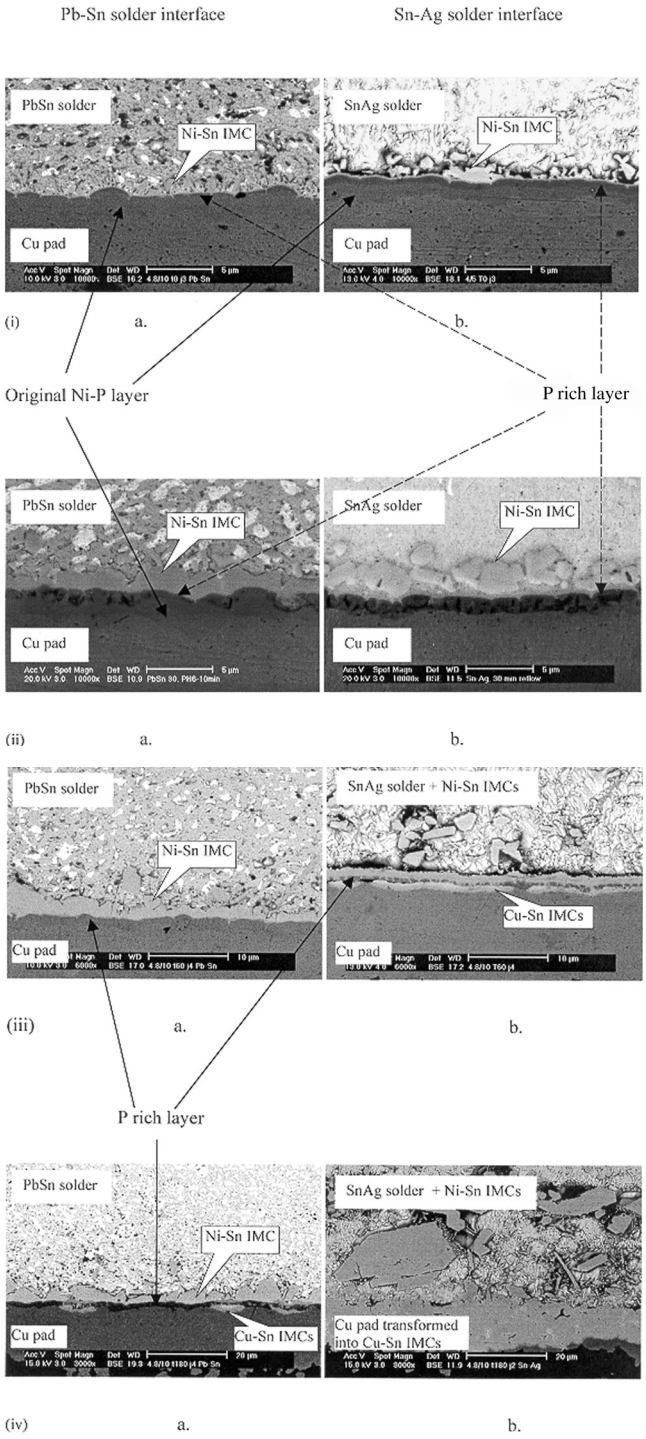

Fig. 2. Backscattered electron micrographs of the solder joint reflowed at (i) 0.5 min, (ii) 30 min, (iii) 60 min, and (iv) 180 min.

analysis of IMC layer/grains reflowed for longer times revealed higher Sn content than the stoichiometric ratio for Ni_3Sn_4. For a 60 min reflow, the IMC layer in the Pb-Sn solder interface (Fig. 2iiia) has started to diffuse out and mix with the liquid solder. The P-rich dark Ni-P layer also becomes thicker with the thinning of the original Ni-P layer. For the Sn-Ag solder (Fig. 2iiib), the Ni-Sn IMC grains spread over a large area of the liquid solder, leaving only a thin continuous layer with the P-rich Ni-P fractured layer. No traces of original Ni-P were detected for a 60 min reflow in Sn-Ag solder. The P-rich Ni-P layer opened numerous channels for Sn to diffuse into the Cu layer. From the figure, patches of two successive layers are clear beneath the P-rich fractured layer on top of the Cu pad. From the EDX analysis, Cu_5Sn_6 and Cu_3Sn compounds were detected in these regions. Choi et al. and Kang et al. also found such Sn diffusion underneath the Ni-Sn IMC into the Cu pad.[19,20]

At the longest reflow time (e.g., 180 min), no Ni-P layer or even Cu pad was observed for the Sn-Ag solder interface (Fig. 2ivb). The Cu pad was consumed by Sn to form Cu_5Sn_6 and Cu_3Sn IMCs, whereas in the Pb-Sn solder, there was still a P-rich dark Ni-P layer with some Cu_5Sn_6 and Cu_3Sn IMCs on top of the Cu pad (Fig. 2iva).

Figure 3 shows the variation of the Ni-P original layer and P-rich dark Ni-P layer with reflow time for both types of solder. The original Ni-P layer decreases and the new P-rich Ni-P layer increases with reflow time; however, the rate of changes is faster for the Sn-Ag solder. The P-rich Ni-P layer diminishes after a 30 min reflow due to the successive consumption of the Ni to form Ni-Sn IMC. Thickness

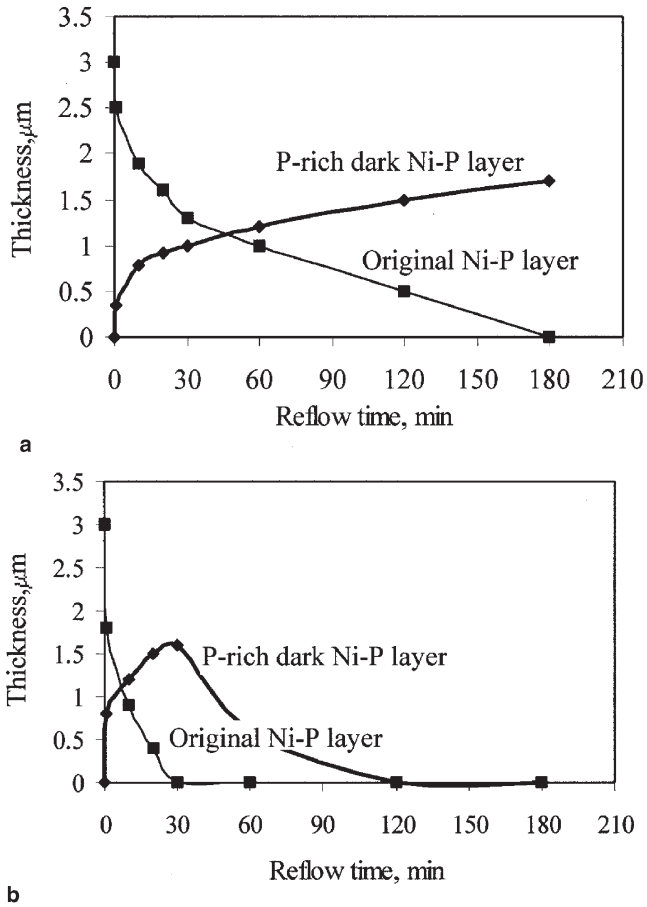

Fig. 3. Growth of the P-rich Ni layer and consequent consumption of the original electroless Ni-P layer. (a) Pb-Sn solder joint, and (b) Sn-Ag solder joint.

of the Ni-Sn IMC layer was not considered for comparison because of the nonadhering characteristics as well as the varying composition of the Ni-Sn IMC layer in the Sn-Ag solder interface. Ni-Sn IMC in the Sn-Ag solder interface was also incorporated with huge P, which might be present as a compound with Ni.

The XRD spectra of the interface layer between electroless Ni-P and the solder joints were collected for both Pb-Sn and Sn-Ag alloys. These interfaces were prepared by reflowing for 60 min at 240°C and etching off the unreacted Sn and Pb to determine the possible compounds formed at the interface.

DISCUSSION

The melting points of eutectic 67Pb-37Sn solder and 96.5Sn-3.5Ag solder are 183°C and 221°C, respectively. The reflow temperature was 240°C. When molten solder comes in contact with the Ni-P layer, the possibility exists of forming intermetallics between Sn and Ni, Sn and P, Pb and Ni, and Pb and P, for Pb-Sn solder, and Sn and Ni, Sn and P, Ag and Ni, and Ag and P, for Sn-Ag solder. However, only Ni-Sn IMCs were observed for both cases. As a result, due to the consumption of Ni to form Ni-Sn IMC, P is expelled to the remaining Ni-P layer and forms a P-rich dark Ni-P layer. The solubility of P in molten Pb/Sn is 0 and no Pb-P/Sn-P compounds are found to form.[21] It was reported previously that after reflow, Ni_3Sn_4 and Ni_3P were formed at the interface of the electroless Ni-P and the eutectic Pb-Sn solder due to solder reaction-assisted crystallization.[12,13]

From the XRD studies, two Ni-Sn compounds (Ni_3Sn_4 and $NiSn_2$) as well as some Ni-P compounds such as Ni_3P, Ni_2P, Ni_5P_4, and NiP_2 were identified.[22] The concentration of P found in the dark P-rich Ni-P layer by EDX varied over a wide range, which agrees with these XRD results that there might be a mixture of the tiny crystals of Ni_3P, Ni_2P, Ni_5P_4, and NiP_2.

The mechanism of the IMC formation is summarized in Fig. 4. During reflow, Sn in the solder reacts very quickly with Au layer. This thin Au layer (0.5 μm) is consumed within 30 sec. Then, a thin layer of Ni_3Sn_4 forms at the solder-electroless Ni-P interface. This Ni_3Sn_4 layer grows with time but at different rates for Pb-Sn solder and Sn-Ag solder—a higher rate for Sn-Ag and a lower rate for Pb-Sn. This is clearly due to the high Sn content in the Sn-Ag solder. A high proportion of liquid Sn in molten Sn-Ag solder can react with the Ni-P layer without any barrier. After a certain thickness is achieved, this Ni-Sn IMC starts to break and particles of $Ni_3Sn_4/NiSn_2$ spall out from the layer to the molten solder. As Ni is being consumed, the thickness of the P-rich crystalline Ni-P layer increases in the upper region of the Ni-P layer. At the same time, the thickness of the original Ni-P layer is reduced. After reaching a certain thickness, the dark Ni-P layer breaks and numerous channels are opened. These channels are the result of the coalescence of the

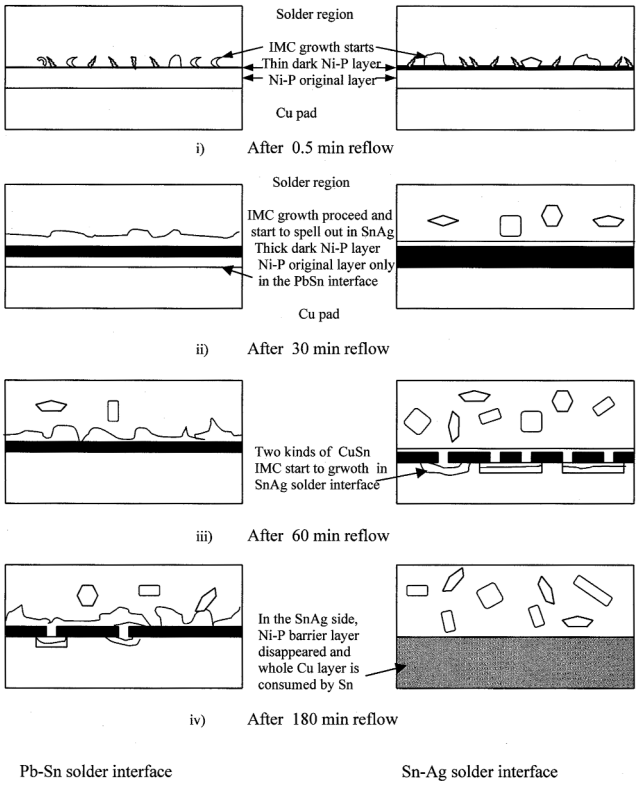

Fig. 4. Schematic diagram showing the changes in the interface region of the Pb-Sn and the Sn-Ag solder with the electroless Ni-P due to longer time reflowing.

Kirkindall voids formed during the diffusion process.[12,16] The Sn comes at a faster rate through these channels to the Cu pad and reacts with Cu to form Cu-Sn IMCs. Two types of Cu-Sn IMCs are found (Cu_5Sn_6 and Cu_3Sn). Cu_3Sn was found adjacent to the Cu pad. The reason for this variation is due to the concentration gradient of Sn to the Cu layer. The Sn diffuses through the channel of the fractured P-rich crystalline Ni-P layer, leaving unreacted Ni. This Ni forms the Ni-P compound, which makes it stable.

The EDX analysis of the dark P-rich crystalline Ni-P layer for Pb-Sn solder revealed 33at.%P and 67at.%Ni. A high content of P was also found in the dark layer by several other authors.[15,23] Zeng et al.[23] claimed the existence of Ni_5P_4 and NiP_3 in the dark layer. Inaba et al.[15] found Ni_2P and NiP_2 at the solder/electroless Ni-P layer. In our previous results,[13] only the Ni_3P layer was detected at a relatively lower reflow temperature (220°C), and it was shown that the Ni_3P layer formed due to the solder reaction-assisted crystallization of electroless Ni-P metallization. Jang et al.[12] found a similar result. We also found Ni_3P compound at the early stages of reflow (0.5 min) at 240°C temperature. After prolonged reflow, different Ni-P compounds formed due to the increase in P percentage in the dark P-rich layer. From our study by XRD, on the sample reflowed at 240°C for 1 h, other NiP compounds such as Ni_5P_4, Ni_2P, and NiP_2 were found along with the

Ni_3P compound. The existence of this Ni_2P compound is also detected by Haseeb et al.[24] by XPS analysis for the 10.2wt.%P content Ni-P layer. Because Ni from the original Ni-P layer was consumed by the Sn of the liquid solder, most of the remaining P diffused to the deeper Ni-P region, and this formed P reached Ni_3P, Ni_2P, Ni_5P_4, and NiP_2 compounds in the dark Ni-P layer. For the Sn-Ag solder, due to the high concentration of Sn, the reaction rate is higher, i.e., $Ni_3Sn_4/NiSn_2$ is formed quickly. All of the P does not get the chance to recede in the deeper Ni-P layer; rather, some rejected P gets entrapped into the $Ni_3Sn_4/NiSn_2$ layer or grains. The rejected P is highly unlikely to be pure P because of the excess of Ni. Extensive EDX studies from this IMC layer near the P-rich Ni-P have been performed to determine the variation of P content and the possible Ni-P compounds. In every case, some P exists in the Ni-Sn IMCs for the Sn-Ag solder.

In the case of the Sn-Ag solder interface, the $Ni_3Sn_4/NiSn_2$ IMCs were found to spread over the solder region in greater extent. This was due to the quicker reaction rate to form $Ni_3Sn_4/NiSn_2$ at mass scale and the entrapment of the P as Ni-P compound—more brittleness was developed than the $Ni_3Sn_4/NiSn_2$ IMCs formed in the Pb-Sn solder interface.

CONCLUSIONS

The original electroless Ni-P layer in this study was found to be amorphous and has a composition of $Ni_{80}P_{20}$. Interfacial kinetics between this electroless Ni-P layer and two different solder materials (Pb-Sn and Sn-Ag) were investigated in terms of dissolution reaction, intermetallic compound growth, and the morphology of the interfacial IMCs. The following conclusions are drawn.

1. The amorphous electroless Ni-P layer crystallized during the reflow process at 240°C in contact with Pb-Sn and also Sn-Ag solder. Different Ni-P compounds such as Ni_3P, Ni_2P, Ni_5P_4, and NiP_2 were identified by EDX and XRD.
2. At the same reflow temperature, the growth rate of Ni-Sn IMC is faster in the Sn-Ag solder than in the Sn-Pb solder. In both cases, two kinds of Ni-Sn IMCs were detected—Ni_3Sn_4 and $NiSn_2$. For the Sn-Ag solder, Ni-Sn IMC was incorporated with P, which is thought to be entrapped due to the rapid reaction of electroless Ni-P layer with Sn-Ag solder.
3. Electroless Ni-P is found to be consumed more rapidly in contact with the Sn-Ag solder. So, the resistance of electroless Ni-P layer as a diffusion barrier of Sn to form Cu-Sn IMCs is lower for the Sn-Ag solder than for the Pb-Sn solder.

This study shows that tiny crystals of Ni_3P, Ni_2P, Ni_5P_4, and NiP_2 are formed from the amorphous electroless Ni-P (20 at.%) due to the successive Ni dissolution during the reflow process. The electroless Ni-P layer is found to have less resistant capacity against the 96.5Sn-3.5Ag solder than against the 37Pb-63Sn solder.

ACKNOWLEDGEMENTS

The authors acknowledge the financial support provided by CERG Project No. 9040621 of the Hong Kong Research Grants Council. The authors are grateful to Mr. M.A. Uddin for his assistance with the SEM analysis.

REFERENCES

1. R.R. Tummala, *Fundamentals of Microsystems Packaging* (New York: McGraw-Hill, 2001), pp. 365–368, 673–676.
2. C.E. Ho, Y.M. Chen, and C.R. Kao, *J. Electron. Mater.* 28, 1231 (1999).
3. *The Workshop on Lead Free Program* (Herdon, VA: National Electronics Manufacturing Initiative Inc., 2001).
4. S.K. Kang et al., *51st Electronic Components and Technology Conf.* (Orlando, FL, USA, 2001), pp. 448–454.
5. T. Taguchi, R. Kato, S. Akita, A. Okuno, H. Suzuki, and T. Okuno, *51st Electronic Components and Technology Conf.* (Orlando, FL, USA, 2001), pp. 675–680.
6. S. Wiese, A. Schubert, H. Walter, R. Dukek, F. Feustel, E. Meusel, and B. Michel, *51st Electronic Components and Technology Conf.* (Orlando, FL, USA, 2001), pp. 890–902.
7. V. Kripesh, Poi-Siong Teo, C.T. Tai, G. Vishwanadam, and Yew Cheong Mui, *51st Electronic Components and Technology Conf.* (Orlando, FL, USA, 2001), pp. 665–670.
8. S.W. Chen and Y.W. Yen, *J. Electron. Mater.* 28, 1203 (1999).
9. Y.C. Chan, A.C.K. So, and J.K.L. Li, *Mater. Sci. Eng.—Part B* 55, 5 (1998).
10. A.C.K. So, Y.C. Chan, and J.K.L. Li, *IEEE Trans. CPMT-Part B* 20, 463 (1997).
11. P.L. Tu, Y.C. Chan, K.C. Hung, and J.K.L. Lai, *Scripta Mater.* 2, 317 (2001).
12. J.W. Jang, P.G. Kim, K.N. Tu, D.R. Frear, and P. Thomson, *J. Appl. Phys.* 85, 8456 (1999).
13. K.C. Hung, Y.C. Chan, C.W. Tang, and H.C. Ong, *J. Mater. Res.* 15, 2534 (2000).
14. C.Y. Lee and K.L. Lin, *Thin Solid Films* 249, 201 (1994).
15. M. Inaba, K. Yamakawa, and N. Iwase, *IEEE Trans. CHMT* 3, 119 (1990).
16. Y. Jeon, K. Paik, K.S. Bok, W.S. Choi, and C.L. Cho, *51st Electronic Components and Technology Conf.* (Orlando, FL, USA, 2001), pp. 1326–1332.
17. T. Liu, D. Kim, D. Leung, M.A. Korhonen, and C.Y. Li, *Scripta Mater.* 35, 65 (1996).
18. A. Maeda, T. Umemura, Q. Wu, Y. Tomita, and T. Abe, *2000 Int. Symp. on Advanced Packaging Materials* (Georgia, USA, 2000), pp. 135–140.
19. W.K. Choi and H.M. Lee, *J. Electron. Mater.* 28 (1999), pp. 1251–1255.
20. S.K. Kang, R.S. Rai, and S. Purushothaman, *J. Electron. Mater.* 25, 1113 (1996).
21. Z. Mei, M. Kaufmann, A. Eslambolchi, and P. Johnson, *48th Electronic Components and Technology Conf.* (Seattle Washington, USA, 1998), pp. 952–961.
22. JCPDS powder diffraction files #04-0851, #08-0430, #34-0501, #03-0953, #17-0225, and #21-0590 (Newton Square, PA: International Center for Diffraction Data, 1997).
23. K. Zeng, V. Vuoring, and J.K. Kivilathi, *51st Electronic Components and Technology Conf.* (Orlando, FL, USA, 2001), pp. 693–698.
24. A.S.M.A. Haseeb, P. Chakraborti, I. Ahmed, F Caccavale, and R. Bertoncello, *Thin Solid Film* 281, 140 (1996).